Development 138, 3319-3330 (2011) doi:10.1242/dev.067645

A-MYB (MYBL1) transcription factor is a master regulator of male meiosis

Ewelina Bolcun-Filas[1,*], Laura A. Bannister[1,2,*], Alex Barash[1], Kerry J. Schimenti[1], Suzanne A. Hartford[1,2], John J. Eppig[2], Mary Ann Handel[2], Lishuang Shen[1] and John C. Schimenti[1,2,†]

SUMMARY

The transcriptional regulation of mammalian meiosis is poorly characterized, owing to few genetic and ex vivo models. From a genetic screen, we identify the transcription factor MYBL1 as a male-specific master regulator of several crucial meiotic processes. Spermatocytes bearing a novel separation-of-function allele (*Mybl1*^{repro9}) had subtle defects in autosome synapsis in pachynema, a high incidence of unsynapsed sex chromosomes, incomplete double-strand break repair on synapsed pachytene chromosomes and a lack of crossing over. MYBL1 protein appears in pachynema, and its mutation caused specific alterations in expression of diverse genes, including some translated postmeiotically. These data, coupled with chromatin immunoprecipitation (ChIP-chip) experiments and bioinformatic analysis of promoters, identified direct targets of MYBL1 regulation. The results reveal that MYBL1 is a master regulator of meiotic genes that are involved in multiple processes in spermatocytes, particularly those required for cell cycle progression through pachynema.

KEY WORDS: Meiosis, Mouse, Cell cycle

INTRODUCTION

Meiosis I is arguably the most complex cell division cycle in eukaryotes. It includes unique events such as: (1) the developmental decision to enter meiosis and activate a specialized developmental program; (2) initiation of recombination via genetically programmed induction of DNA double-strand breaks (DSBs), which (in most organisms) drives pairing of homologous chromosomes; (3) recombinational repair of DSBs via crossover and non-crossover recombination pathways; (4) monitoring of the above events by checkpoint systems; (5) targeting a set number of DSB repair events to a crossover recombination pathway that is important for balanced segregation of chromosomes at the first meiotic division; and (6) execution of a reductional cell division. Failure to execute properly one or more of these events causes meiotic defects, which in turn can lead to infertility or birth defects. Such complexity requires tightly coordinated gene expression. Moreover, these processes are sexually dimorphic: regulated differently in oocytes and spermatocytes.

In *S. cerevisiae*, genetic and molecular studies have led to a comprehensive understanding of meiotic transcriptional regulation (Kassir et al., 2003). The 'master regulator' of yeast meiosis is Ime1, which enables entry into, and progression of, the meiotic cell cycle by activating genes required for premeiotic DNA synthesis, recombination and synapsis. Among the genes activated are other transcription factors required for subsequent events, including meiotic divisions and spore formation. Whereas mammals have conserved homologs of genes that are involved in recombination and synapsis, there are no clear orthologs of the key transcriptional regulatory genes (Handel and Schimenti, 2010). It is possible that mammals employ different and unrelated regulatory factors and mechanisms.

Forward genetic screens enable unbiased discovery of genes that function in a particular process. We have conducted chemical mutagenesis screens in mice to identify novel alleles that cause infertility (Ward et al., 2003; Handel et al., 2006). Here, we report the identification of the first allele from these screens that exhibits specific meiotic defects associated with deficiency for a transcriptional regulatory protein: A-MYB (MYBL1).

MYB (myoblastosis) proteins are nuclear DNA-binding proteins that act as transcriptional transactivators of many genes (Ganter et al., 1999; Ganter and Lipsick, 1999; Oh and Reddy, 1999). They bind and transcriptionally stimulate target genes that regulate cell cycle progression, differentiation and apoptosis (Oh and Reddy, 1999; Sala, 2005). There are three Myb paralogs in mammals: *A-Myb*, *B-Myb* and C-*Myb* (in mice, *Mybl1*, *Mybl2* and *Myb*, respectively). Orthologs of all three are present in vertebrates, while *Drosophila melanogaster* and sea urchins have a single homolog (*Myb*) (Lipsick et al., 2001). Analysis of *Myb* mutant flies implicates a role in mitotic cell cycle progression and, more specifically, in chromosome condensation (Manak et al., 2007).

Mybl1 is highly transcribed in spermatocytes after meiotic entry (Takahashi et al., 1995; Latham et al., 1996; Shima et al., 2004; Su et al., 2004). Furthermore, mice homozygous for a targeted null allele of *Mybl1* exhibit male infertility, abnormal mammary gland development and decreased fitness (Toscani et al., 1997). The male infertility is due to arrest of meiosis at about the pachytene stage, as judged histologically. Therefore, it is possible that MYBL1 is a key regulator of meiosis in spermatocytes.

The allele described herein results in infertility but not in somatic phenotypes, and we identify cytological defects and molecular causes that underlie meiotic arrest in pachynema. Genomic analyses revealed collections of genes directly and indirectly regulated by MYBL1. These genes are involved in key aspects of

[1]Cornell University College of Veterinary Medicine, Department of Biomedical Sciences, and Center for Vertebrate Genomics, Ithaca, NY 14850, USA. [2]The Jackson Laboratory, Bar Harbor, ME 04609, USA.

*These authors contributed equally to this work
[†]Author for correspondence (jcs92@cornell.edu)

Accepted 18 May 2011

meiotic chromosome metabolism, but, most importantly, the key role of MYBL1 appears in meiotic cell cycle control. Additionally, the meiotic transcription of many genes whose products are required postmeiotically is dependent upon MYBL1. Overall, these studies demonstrate that MYBL1 is a master regulator of the male meiotic cell cycle and transcriptional program.

MATERIALS AND METHODS

Mice, mutagenesis and genetic mapping

Male C57BL/6J (B6) mice were mutagenized with ethylnitrosourea (ENU) as described (Wilson et al., 2005), then bred to C3HeB/FeJ (C3H) females to create 'G_1' male founders of pedigrees. These males were backcrossed to C3H females, and G2 daughters were backcrossed to the G_1 male to yield G_3 offspring that were tested for infertility (Lessard et al., 2004). DNA was isolated from infertile G_3 animals in the *repro9* pedigree, and a genome scan was performed with microsatellite markers polymorphic between C3H and B6.

Once linkage was obtained, the mutation-bearing chromosome was propagated by backcrossing into both C3HeB/FeJ (C3H) and Cast/Ei genetic backgrounds for the purposes of positional cloning. The majority of mutant reproductive phenotypic analyses were conducted on male and female animals semi-congenic in the C3H background. The *Mybl1* knockout mice were on a mixed 129 × B6 background.

Affymetrix microarray analysis

Total testis RNA was extracted from homogenized paired testes of wild-type and mutant (at least three) male mice at 14 and 17 dpp using the Qiagen RNAeasy mini kit. RNA was assessed for quality using an Agilent Bioanalyzer 2100. Total RNA from each animal was reverse-transcribed into double-stranded cDNA, which was then in vitro transcribed into biotin-labeled cRNA using GeneChip IVT labeling kit (Affymetrix, Santa Clara, CA). Labeled cRNA was hybridized to Affymetrix mouse genome 430 2.0 GeneChips containing ~ 22,000 genes (45,101 probes) and hybridization signals were read using a GeneChip scanner 3000 (Affymetrix, Santa Clara, CA). The raw data was processed using Affymetrix GCOS software to obtain detection calls and signal values. The signals of each array were scaled to a target value of 500 using GCOS and Bioconductor. Two-way ANOVA analysis was carried out to resolve those genes that were differentially expressed either between genotypes and/or days using MeV (version 4.6.1) on $\log_2$-transformed expression values. Results were multiple test corrected with the Benjamini-Hochberg method to control the false discovery rate (FDR) in R. About 800 genes significant at FDR ≤0.025 were selected as differentially expressed (DE) for downstream analysis. DE genes were analyzed with the Limma package (Smyth, 2004). A change of at least twofold was used to define a DE gene. The microarray data presented in this paper have been deposited to GEO database (Gene Expression Omnibus, http://www.ncbi.nlm.nih.gov/geo/) under Accession Number GSE28025.

Immunocytology

Chromosome spreads from males and females were prepared and immunolabeled as described (Reinholdt et al., 2004), as were squash preparations of seminiferous tubules (Kotaja et al., 2004). The primary antibodies used in this study were as follows: mouse anti-SCP3 (1:500; Abcam); rabbit anti-SYCP1 (1:1000; a gift from C. Heyting, Wageningen University, The Netherlands); rabbit anti-RAD51 (1:250, this polyclonal antibody recognizes both RAD51 and DMC1; Oncogene Research Products); rabbit anti-γH2AX (1:500; Upstate Biotechnology; rabbit anti-MLH3 (1:400; a gift from P. Cohen, Cornell University, Ithaca, NY, USA); mouse-anti-human MLH1 (1:50; BD Biosciences); mouse-anti-ubiquityl-histone H2A (1:200; Upstate Biotechnology); human CREST serum (1:2000; a gift from W. Brinkley, BCM, Houston, TX, USA); guinea pig anti-H1t (1:2000; a gift from M. A. Handel, The Jackson Laboratory, Bar Harbor, ME, USA); rabbit anti-SUMO-1 (1:250; Cell Signaling); rabbit anti-SUMO-2/3 (1:250; Cell Signaling); and rabbit anti-MYBL1 (1:250; Sigma Prestige Antibodies). Secondary antibodies used were Alexa Dye (AlexaFluor-488, 594 and 647) conjugates (Molecular Probes) at 1:1000 dilutions. Images were taken with an Olympus BX51 microscope at 60× or 100× magnification. For histological analyses, testes and ovaries were dissected and fixed in Bouin's, embedded in paraffin, sectioned and stained with Hematoxylin and Eosin.

Western blotting

Testicular extracts (50 μg) from wild-type and mutant testes were electrophoresed in 10% SDS/PAGE gels and then electroblotted to Trans-Blot nitrocellulose membranes (BioRad). After blocking with 5% non-fat milk in TBST (Tris-Buffered Saline Tween-20), membranes were incubated with rabbit anti-MYBL1 (1:500; Sigma Prestige Antibodies) or mouse anti-α-tubulin (1:2000; Sigma Aldrich), followed by HRP-conjugated secondary antibodies. Signal was detected using a Pierce ECL western blotting substrate detection kit.

ChIP-chip

For chromatin immunoprecipitation (CHIP) and subsequent steps, we used Nimblegen's sample preparation protocol with some modifications. Briefly, juvenile testes were dissected and seminiferous tubules were minced in RPMI media (Invitrogen) to release cells. Tubule remnants were removed by centrifugation and testicular cells were fixed with formaldehyde (1% v/v) for 10 minutes on ice. Crosslinking was stopped with 125 mM glycine for 5 minutes. The cell suspension was washed three times in PBS and lysed with SDS-lysis buffer [1% SDS, 10 mM EDTA, 50 mM Tris-HCl (pH 8.1)] for 15 minutes on ice, then dounced 5-10 times. Chromatin was fragmented to an average DNA length of 300-500 nucleotides by sonication (5×30 seconds). Prior to ChIP, the extract was diluted 10-fold in 0.01% SDS, 1.1% Triton X-100, 1.2 mM EDTA, 16.7 mM Tris (pH 8.1), 167 mM NaCl and 11% glycerol. Chromatin extracts were immunoprecipitated with rabbit anti-MYBL1 antibodies (Sigma Prestige Antibodies). Following immunoprecipitation, MYBL1-bound DNA fragments were eluted and amplified using a WGA2 GenomePlex Complete Whole Genome Application (WGA) kit (Sigma Aldrich) according to the manufacturer's protocol. Input and ChIPed DNA fragments were labeled and hybridized to Nimblegen 385K RefSeq Promoter arrays following manufacturer's recommendations (two replicates). After hybridization and scanning, the raw intensities were exported from NimbleScan (v2.5) in NimbleGen's pair format into Ringo (Toedling et al., 2007). Statistical analysis for ChIP-chip data were conducted with the Ringo package, which includes quality assessment, data normalization and transformation, and the calling of regions of interest. The standard pre-processing method suggested by NimbleGen for ChIP-chip was used to compute the log ratios log2(Cy5/Cy3) for all probes with Tukey's biweight mean scaling method to adjust for systematic dye and labeling biases. The probe intensities were smoothed with a 600 bp sliding window along the chromosome considering the size distribution of DNA fragments after sonication and the average spacing between probes. The ChIP-enriched Regions (peaks) were identified requiring at least three supporting probes having smoothed intensities exceeding the enrichment threshold. The threshold was chosen individually for each sample with a mixture modeling approach assuming 1% of probes on the array that are expected to show enrichment.

The peaks were annotated with nearby neighboring genes using NimbleScan (V2.5). The DNA sequences from ChIP peak regions were extracted from C57BL/6J reference genome Build 37. The motifs in the sequences were identified with MATCH at the Biobase/Gene Regulation web server (www.biobase-international.com). As background, 10,000 probe sequences were fed to MATCH, and the motif frequency and classification were used as background control frequency of each motif to identify over (or under)-representation motifs in peaks using *P*-values based on Fisher's Exact Test.

For analyzing overlap between *Mybl1*-ChIPed and *repro9* differentially expressed genes individual IDs for each platform (Affymetrix 438 2.0 and Nimblegen 385K RefSeq arrays) were linked to the corresponding UniGene and Entrez Gene IDs using annotation files provided by Affymetrix and Nimblegen. Replicates were removed and only individual genes with unique identifiers were evaluated. UniGene and Entrez Gene IDs were used as variables to calculate overlap between the two platforms as well as between ChIPed and *repro9* DE genes. The Affymetrix array

contains 45,101 probes representing 21,758 unique genes. The Nimblegen chip contains probes for 18,200 unique genes; however, only 15,164 of them were present on both platforms. Affymetrix IDs from DE genes, ChIP peaks and various intersections between them were analyzed with the DAVID Functional Annotation Tool for gene ontology and pathway analysis (http://david.abcc.ncifcrf.gov/) (Huang da et al., 2009; Sherman et al., 2007). Overlap statistical significance was calculated using web-based hypergeometric distribution calculator designed by Jim Lund (University of Kentucky, Lexington, KY, USA) (http://nemates.org/MA/progs/overlap_stats.html). A representation factor below 1.0 indicates under-representation, whereas a value above 1.0 indicates over-representation.

RESULTS

Isolation of the *repro9* infertility allele

We identified a recessive, male-specific infertility mutation, *repro9*, in a large-scale ENU mutagenesis program to identify alleles causing mouse infertility (http://reproductivegenomics.jax.org/) (Handel et al., 2006). *repro9/repro9* males failed to impregnate wild-type female partners, and upon clinical examination, were found to have small testes and no epididymal sperm. Testis histopathology revealed that, in contrast to wild-type adult seminiferous tubules (Fig. 1A), mutants lacked postmeiotic spermatids (Fig. 1B). The most developmentally advanced germ cells in the mutants had chromatin morphology characteristic of the pachytene stage of meiosis (Fig. 1B). The block in meiotic progression was evident from the first wave of spermatogenesis. Although control seminiferous tubules contained round spermatids at 22 days postpartum (Fig. 1A, inset) mutant tubules did not, exhibiting spermatocytes with pachytene-like chromosomes and many adluminal cells with apoptotic/pyknotic nuclei (Fig. 1B, inset).

Unlike mutant males, homozygous *repro9* females under 6 months of age exhibited normal ovarian histology, were fully fertile with an average litter size of 7.42±0.5 versus 7.5±0.5 in heterozygous controls, and successfully raised their young (see Fig. S1 in the supplementary material). Mutant mice of both sexes were of normal stature and exhibited no other apparent morphological defects.

repro9 is an allele of the transcription factor gene *Mybl1*

The *repro9* mutation was mapped genetically to a ~6 Mb centromere-proximal region on chromosome 1 that contained an obvious candidate gene, *Mybl1* (myeloblastosis oncogene-like 1). Mice homozygous for a gene-targeted *Mybl1* allele exhibit male-specific infertility, with an arrest of spermatogenesis in meiosis (Toscani et al., 1997). However, whereas *Mybl1*$^{-/-}$ mice are runted and females fail to nurse their young, owing to defects in mammary tissue differentiation during pregnancy, *repro9* mutants have neither phenotype. Nevertheless, the similarity in the male reproductive phenotypes prompted us to sequence the *Mybl1* allele associated with *repro9*. No marked differences in *Mybl1* expression were observed using PCR analysis of cDNA derived from wild-type and mutant testis RNA with several primer pairs spanning the *Mybl1*-coding sequence (data not shown). However, genomic sequencing revealed a *de novo* mutation in exon 6 in all mice bearing *repro9* (Fig. 1F). The mutant allele contains a C to A transversion at nucleotide 893 of the *Mybl1* mRNA (RefSeq NM_008651).

The 751 amino acid MYBL1 protein (NP_032677) shares substantial homology with its two paralogs MYBL2 and MYB. They all contain a highly conserved N-terminal DNA-binding domain consisting of three tandem 50 amino acid repeats, a

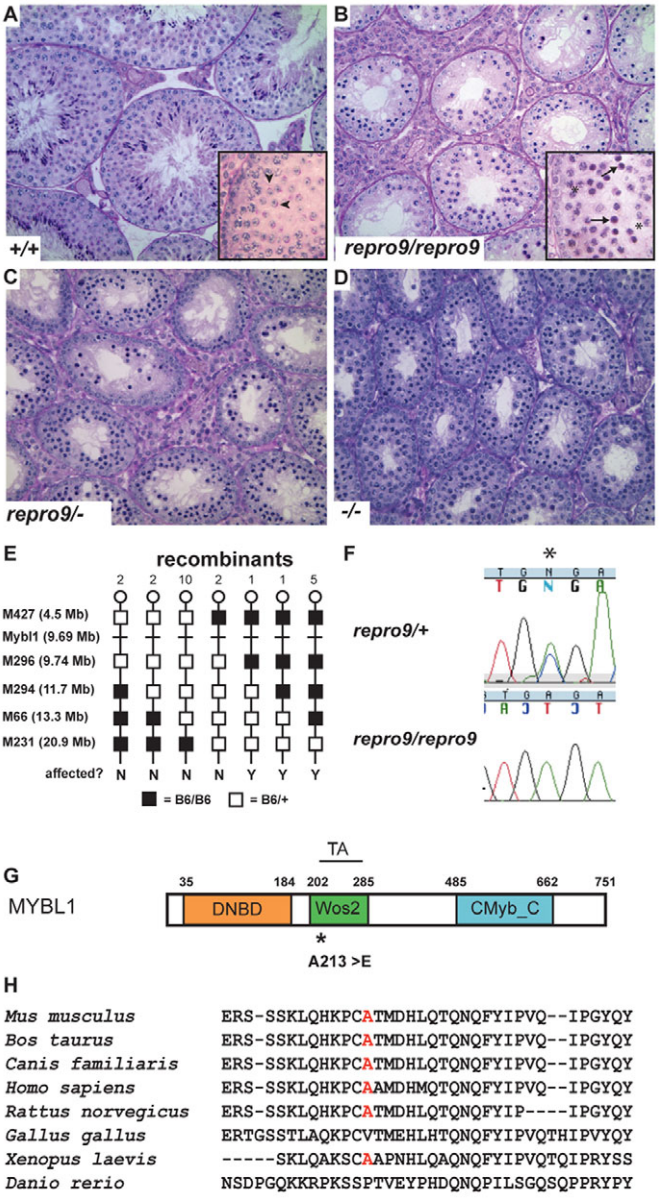

Fig. 1. *repro9* mutant males display meiotic arrest caused by a mutation in *Mybl1*. (**A-D**) Hematoxylin and Eosin-stained testis sections of wild-type (A), *repro9/repro9* (B), compound heterozygous *repro9*/*Mybl1*$^{-}$ (C) and *Mybl1*$^{-/-}$ (D) adult males (original magnification was 40×). Insets in A and B show higher magnification of a PAS-stained seminiferous tubule from 22 dpp *repro9*/+ and *repro9/repro9* littermates, respectively. The arrowheads indicate forming acrosomes (red stained) of round spermatids in a control. Some mutant spermatocytes have progressed to pachynema (asterisks in B, insert) and others are apparently undergoing apoptosis (arrows). The *Mybl1*$^{-}$ allele fails to complement *repro9* (C) and adult *Mybl1*$^{-/-}$ mutants show meiotic arrest similar to *repro9* (D). (**E**) Positional cloning of *repro9* identifies a mutation in *Mybl1*. Recombinant haplotypes on proximal mouse Chr 1 were mapped using microsatellite loci as indicated by boxes. (**F**) Sequence traces of indicated genotypes showing C to A mutation (asterisk). (**G**) Schematic diagram of MYBL1 domains. DNBD, Myb-like DNA-binding domain; Wos2 domains are associated with transcriptional regulation; TA, transactivation domain; Cmyb_C: C-terminal negative regulatory domain. (**H**) Partial amino acid sequence alignment surrounding the site of the A213E mutation in various MYBL1 homologs. Mutated alanine 213 is indicated in red.

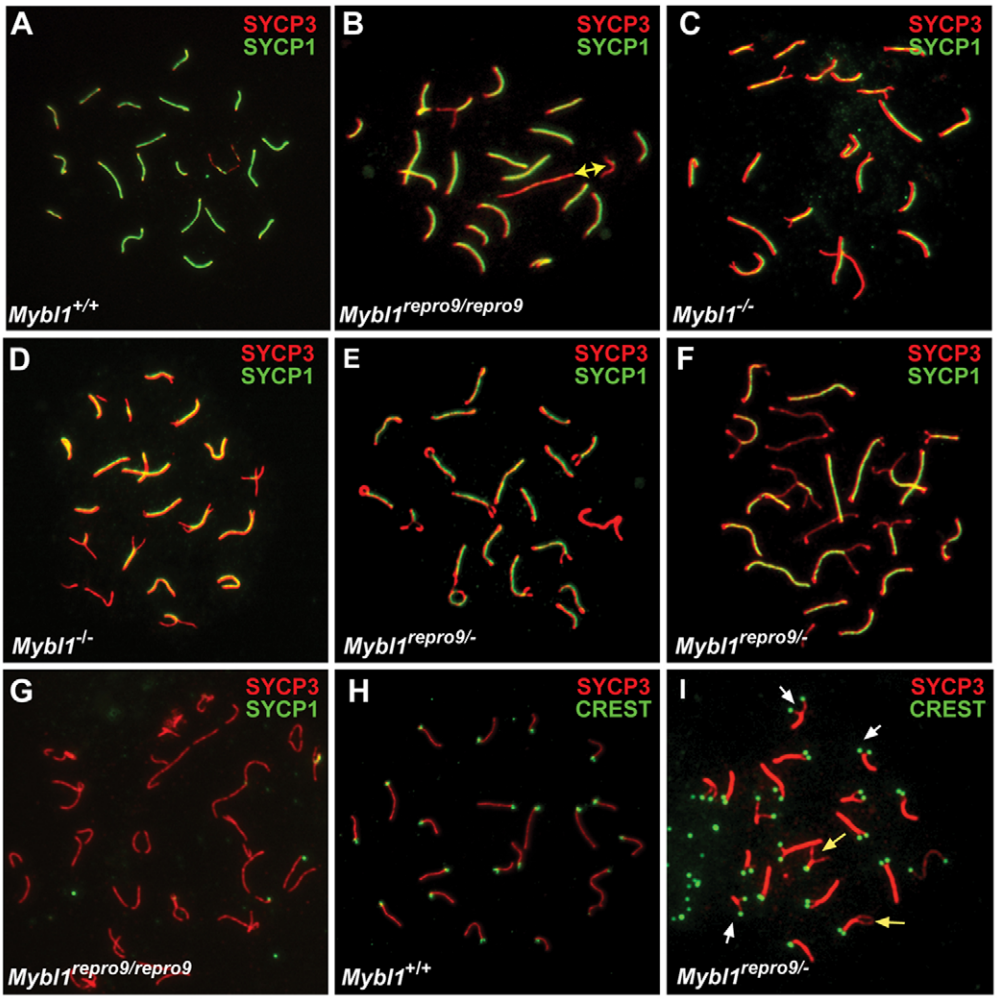

Fig. 2. *Mybl1* mutant spermatocytes show minor synapsis defects of the XY pair and autosomal termini. (**A-I**) Surface spread spermatocyte nuclei were immunostained with the anti-SYCP3 and anti-SYCP1 antibodies, to detect AEs and CEs, respectively. CREST serum labels centromeres. The yellow double-headed arrow in B indicates the presumptive XY pair. White and yellow arrows in I indicate peri-centromeric and opposite end asynapsis, respectively. Genotypes are indicated, with a minus indicating the null allele.

transactivation domain and a regulatory domain in the C-terminal region of the protein (Fig. 1G) (for a review, see Oh and Reddy, 1999). The *Mybl1* mutation in *repro9* (henceforth designated $Mybl1^{repro9}$) results in a nonconservative amino acid change from alanine at position 213 to glutamic acid (A213>E). This evolutionarily conserved residue lies near the N-terminal border of the functionally defined transactivation domain (Takahashi et al., 1995). Most of this region (239-285 amino acids) is also annotated by Pfam as a Wos2 domain (PF07988) that is associated with transcriptional regulation (Fig. 1G). The alteration of a neutral and hydrophobic amino acid to charged and hydrophilic amino acid raised the possibility that the mutation is deleterious, possibly with respect to the function of MYBL1 as a transcriptional activator, and therefore represents the causative *repro9* mutation.

To determine whether the $Mybl1^{repro9}$ allele underlies the reproductive phenotype, a complementation test was performed with the null allele (Toscani et al., 1997). All three $Mybl1^{repro9}/Mybl1^{-}$ males tested were sterile with a testis histopathological phenotype indistinguishable from that of $Mybl1^{repro9}$ and $Mybl1^{-}$ homozygotes (Fig. 1B-D); that is, no postmeiotic spermatids were present, and the most advanced germ cells were at the pachytene stage. Progression of spermatogenesis was arrested at epithelial Stage IV, equivalent to mid-pachynema in wild type, which is typical of diverse mouse meiotic mutants (Barchi et al., 2005). Additionally, as described below, meiotic chromosome abnormalities were identical between the compound heterozygotes and either of the homozygous mutants. However, $Mybl1^{repro9}$ homozygotes did not exhibit runting or abnormal breast development, as did homozygous null mice (see Fig. S2 in the supplementary material) (Toscani et al., 1997), indicating that $Mybl1^{repro9}$ is a hypomorphic or separation-of-function allele that specifically impairs the spermatogenesis function of MYBL1.

MYBL1-deficient spermatocytes exhibit aberrant synapsis of the sex chromosomes and chromosome termini during pachynema

To identify the basis for meiotic arrest in $Mybl1^{repro9/repro9}$ and $Mybl1^{repro9/-}$ testes, we immunolabeled surface-spread spermatocyte nuclei with antibodies against axial/lateral (SYCP3) and central (SYCP1) elements of the synaptonemal complex. Pachytene chromosome cores from $Mybl1^{repro9/repro9}$ spermatocytes were generally of normal length and appearance, and many

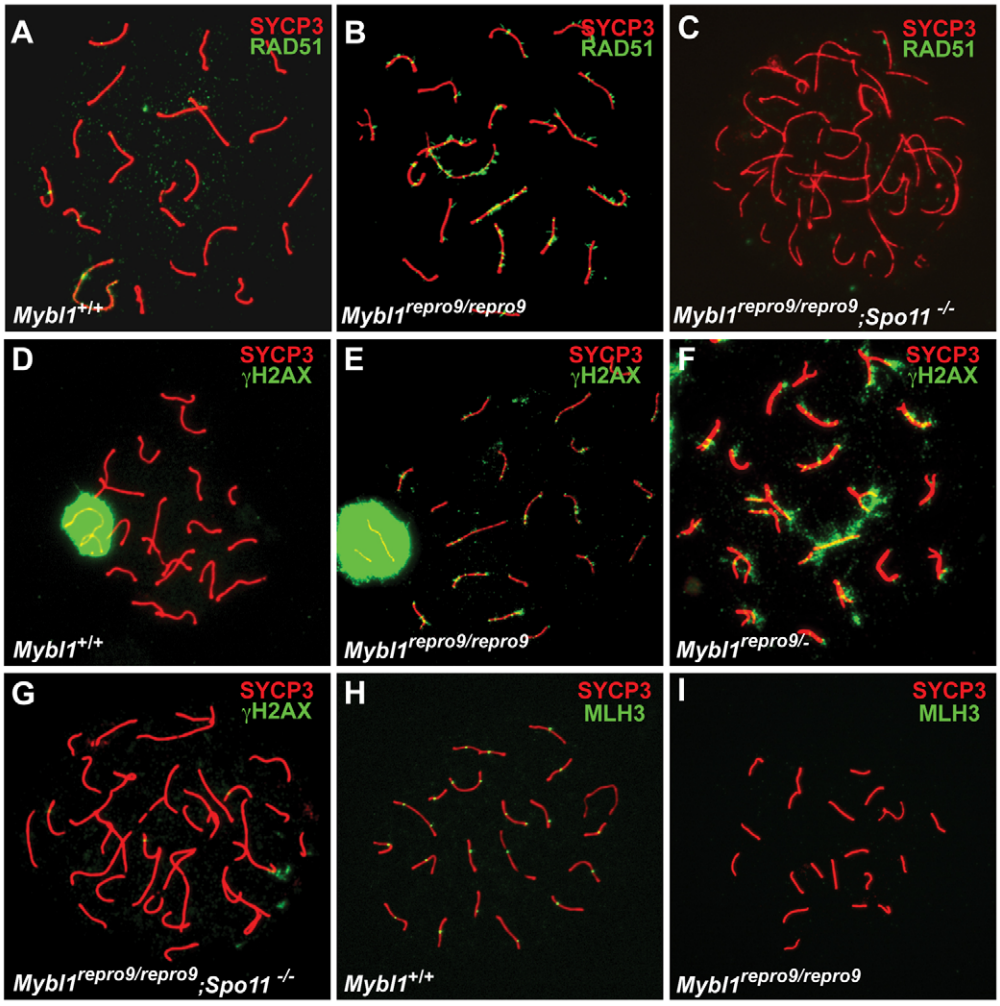

Fig. 3. DSBs are inefficiently repaired and crossovers fail to form in *Mybl1* mutant spermatocytes. (**A-I**) Surface spread spermatocyte nuclei were immunostained for indicated proteins. *Mybl1* mutant spermatocytes show persistent DSBs (B,E,F) and lack of MLH3 foci (I) in pachynema. All spermatocytes are pachytene, except for C and G, which are in zygonema/pachynema (as defined by state of chromosome synapsis) due to the *Spo11* mutation. Genotypes and antibodies used for immunostaining are indicated.

spermatocytes contained a complement of fully synapsed bivalents, including an XY pair synapsed at the pseudoautosomal region (see Fig. S4B in the supplementary material). However, 51.2% of *Mybl1*$^{repro9/repro9}$ pachytene nuclei were aberrant; they failed to maintain or establish synapsis of homologous autosomes at terminal regions (20.4%), and/or exhibited XY asynapsis (20.8%; compare wild type with mutant in Fig. 2A,B). *Mybl1*$^{repro9/-}$ and *Mybl1*$^{-/-}$ spermatocytes exhibited similar (Fig. 2C), if not more severe meiotic chromosome defects (Fig. 2D,E). These synaptic defects are male specific; we did not observe such abnormalities in *Mybl1*$^{repro9/repro9}$ oocytes (see Fig. S3 in the supplementary material). These observations provide the first cytological basis for meiotic arrest and consequent infertility in *Mybl1*$^{-/-}$ mice, and further confirm that *repro9* is an allele of *Mybl1*.

Although many mutant spermatocytes display normal chromosome synapsis and some reach mid- or late-pachynema, as judged cytologically by synapsis of the XY bivalent (quantified above; see Fig. S4B in the supplementary material), we did not observe typical late diplotene nuclei with a complement of bivalents attached by chiasmata. Rather, we observed rare nuclei with meiotic core morphology resembling either early diplonema, with knob-like structures at chromosome termini (Fig. 2F), or late diplonema with closely opposed similarly sized SYCP1-free chromosomes that lack physical attachments (Fig. 2G), which suggests failure to establish/maintain crossovers and homolog associations. Since histological analyses indicated Stage IV (mid-pachytene) arrest of the seminiferous epithelium, and no metaphase I spermatocytes were observed, it is likely that there is a slight disconnect between chromosomal dynamics and developmental progression of spermatocytes, and this might be a consequence of the range of defects showed by individual spermatocytes. This is addressed below using cell cycle markers.

The majority of synaptic defects involved chromosome termini and the XY bivalent. To determine whether the terminal asynapsis occurs preferentially on the centromeric or distal ends (mouse chromosomes are telocentric), we immunolabeled spermatocyte nuclei with CREST antiserum and anti-TRF2, which detect centromeric heterochromatin and telomeres, respectively. CREST labeled all mutant and wild-type chromosomes (Fig. 2H,I). In terminally asynaptic chromosomes, the majority of asynapsis (88.4%, n=155 chromosomes) occurred peri-centromerically (resulting in dual CREST foci) with the rest occurring at the

opposite ends of the chromosomes (8.4%) (Fig. 2I, white and yellow arrows, respectively) or at both ends (3.2%). In addition, both synapsed and unpaired regions of mutant chromosome cores stained positively for cohesins REC8 (Fig. 4E,F) and STAG3 (not shown), indicating that the synaptic defects were not driven by loss of sister chromatid or homolog cohesion at chromosome termini.

Mutant spermatocyte nuclei have persistent unrepaired double strand breaks (DSBs) and lack crossing over

That mutant chromosomes underwent substantial synapsis suggested that a recombination-driven homolog search drove chromosome pairing, and that assembly of critical SC elements was grossly unaffected. However, the failure to establish completely or to maintain full synapsis implied possible defects in recombination-driven physical attachments of homologous chromosomes. To explore these possibilities, we assessed the distribution of key recombination repair proteins.

Mutant zygotene spermatocytes had a typical distribution of RAD51 foci, indicating that meiotic DSBs were induced and recombinational repair was initiated (see Fig. S4A in the supplementary material). However, whereas these foci almost completely disappear in mid-pachytene wild-type spermatocytes (Fig. 3A), mutant nuclei contained persistent RAD51 foci along meiotic cores in both synapsed and asynapsed regions (Fig. 3B; see Fig. S4A in the supplementary material). Similarly, γH2AX foci persisted abnormally on synapsed regions of mutant pachytene chromosomes (compare wild type in Fig. 3D with 3E). In mid-late mutant pachytene nuclei with extensive asynapsis, γH2AX was present both as foci on synapsed cores and as cloud-like staining over asynapsed chromosome regions (Fig. 3F). The cloud-like staining may be due to the MSUC (meiotic silencing of unsynapsed chromatin) response, in which ATR phosphorylates H2AX, whereas the foci are likely to mark ATM-mediated H2AX phosphorylation that occurred earlier in response to meiotic DSBs (Turner et al., 2004; Turner et al., 2006). Zygotene/pachytene spermatocytes from *Mybl1*$^{repro9/repro9}$, *Spo11*$^{-/-}$ compound mutants lacked RAD51 and γH2AX foci (Fig. 3C,G), supporting the conclusion that unrepaired DSBs persist in MYBL1-deficient pachytene spermatocytes. Significantly, mutant cores lacked MLH3 (Fig. 3H versus 3I) that mark chiasmata (Lipkin et al., 2002; Marcon and Moens, 2003), indicating that crossing over does not occur. The presence of unrepaired DSBs and lack of meiotic crossovers is specific to mutant males, as *Mybl1*$^{repro9/repro9}$ females exhibited normal appearance and disappearance of early recombination nodules, and had a typical distribution of MLH3 foci (see Fig. S3 in the supplementary material).

Mybl1 mutant spermatocytes exhibit abnormal cell cycle progression

The progression of wild-type meiocytes through substages of prophase I is formally defined by the status of chromosome alignment and synapsis. In *repro9* mutants, both processes are often compromised; hence, it is difficult to assess meiotic progression precisely. To determine whether the meiotic developmental program progresses past mid-pachynema in *Mybl1* mutant spermatocytes, we assessed presence of histone H1t, a mid-pachynema marker (Inselman et al., 2003). Whereas wild-type spermatocytes at mid/late pachytene and diplotene stages exhibited abundant H1t protein (Fig. 4A), *Mybl1*$^{repro9/repro9}$ spermatocytes did not, despite having a cytological appearance of normal mid/late pachytene cells (Fig. 4B).

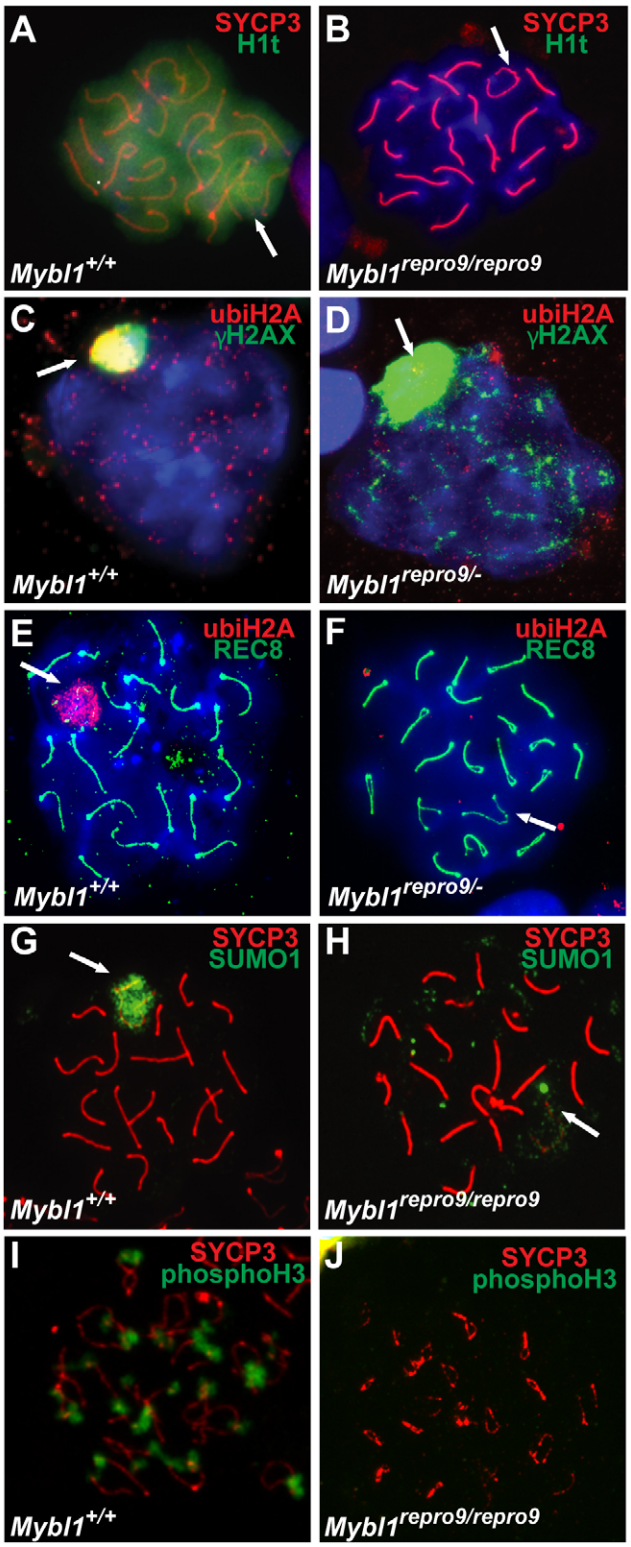

Fig. 4. Abnormal expression of meiotic cell cycle markers in *Mybl1* mutant spermatocytes. (**A-J**) Surface spread pachytene spermatocyte nuclei were immunostained for known markers of meiotic progression. Lack of histone H1t (B) and ubiquitylated histone H2A in the sex body of pachytene spermatocytes (D,F) suggest arrest prior to mid-pachynema. Mutant spermatocytes also fail to accumulate SUMO1 in the XY body (H), unlike wild type (G). Lack of H3 phosphorylations in mutant spermatocytes confirms arrest prior to diplonema (J). Arrows indicate the XY bivalent.

To further evaluate meiotic progression, we assessed ubiquitylation of histone H2A in XY chromatin, which normally occurs in mid-late pachynema after H2AX phosphorylation. Both marks are also associated with MSUC (Baarends et al., 2005). H2A ubiquitylation was not observed in *Mybl1*$^{repro9/-}$ spermatocytes either in the sex chromatin of γH2AX-positive nuclei (Fig. 4C,D) or in nuclei with asynapsis of chromosome termini or the XY pair (Fig. 4F). Additionally, most mutant spermatocytes showed very weak or no SUMO1 signal in the XY body (Fig. 4H), which typically accumulates sumoylated and SUMO pathway proteins (Fig. 4G) (Rogers et al., 2004; La Salle et al., 2008). However, SUMO2/3 staining appeared to be less affected (not shown). Transition from pachynema to diplonema in normal meiosis is marked by phosphorylation of histone H3 (Cobb et al., 1999). *Mybl1*$^{repro9/repro9}$ testes lacked phosphoH3-positive spermatocytes, suggesting developmental arrest prior to diplonema (Fig. 4I,J). Taken together, these results indicate either that *Mybl1*$^{repro9/repro9}$ spermatocytes arrest developmentally before the mid-pachytene transition, or that MYBL1 is directly or indirectly required for expression of these modified proteins or proteins that modify them.

Expression of MYBL1 in spermatogenesis

To better understand the relationship between MYBL1 and the recombination phenotypes, we characterized the appearance of MYBL1 protein in spermatogenesis. Western blot analysis revealed reduced but not absent MYBL1^{repro9} in mutant testes (Fig. 5A). This could result from protein instability or abnormal testis cellularity. To address this, other meiotic mutants were analyzed. MYBL1 is weakly expressed in DSB-deficient and asynaptic *Mei1* (Fig. 5A) mutants that undergo meiotic arrest at zygonema. *Sycp2*, *Sycp3* and *Dmc1* mutant meiocytes form DSBs but fail to repair them (*Dmc1*) or to synapse normally (*Sycp2*, *Sycp3* and *Dmc1*). All three arrest at the zygotene/pachytene transition but express MYBL1, as do crossover-defective *Ccnb1ip1*$^{mei4/mei4}$ mice that progress to about the same stage as *Mybl1*$^{repro9/repro9}$ (Ward et al., 2007). These analyses point to decreased stability of MYBL1^{repro9}. Western blot analysis of wild-type pre-pubertal testes protein demonstrated that MYBL1 first appears at 12 dpp, coincident with the earliest emergence of pachytene spermatocytes (Fig. 5B). Immunolabeling of intact germ cells revealed robust nuclear MYBL1 in mid-late pachytene and diplotene spermatocytes, but not in less mature late zygotene/early pachytene cells (Fig. 5C,D). The combined results indicate that MYBL1 appears robustly at the onset of pachynema.

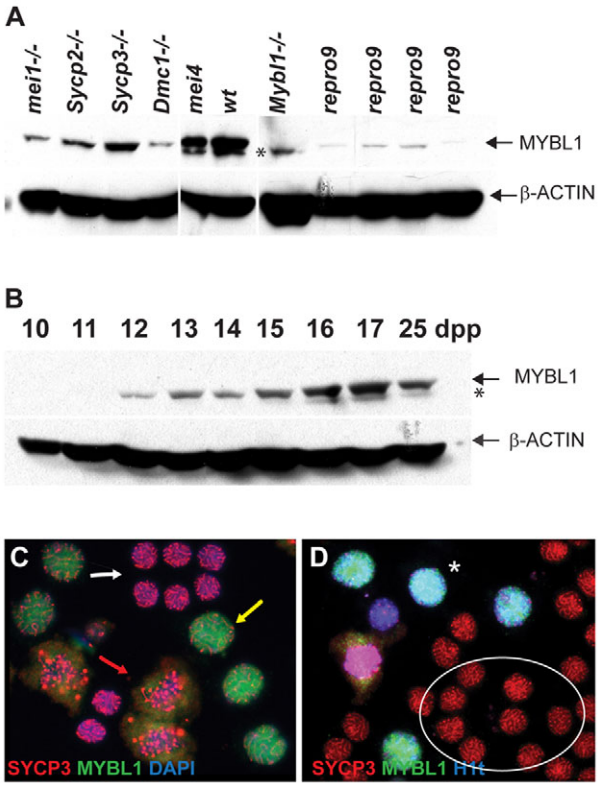

Fig. 5. MYBL1 expression in the testis. (**A**,**B**) Western blot of total protein lysates from wild-type and mutant testes (A) and juvenile testes from day 10-25 postpartum mice (B) probed with indicated antibodies. Asterisk indicates non-specific species. (**C**,**D**) Testicular squash prep immunostaining. MYBL1 is not present in smaller late zygotene/early pachytene spermatocytes (C; white arrow) but is easily detectable in larger mid/late pachytene (yellow arrow) and diplotene (red arrow) spermatocytes, the identity of which is facilitated by staining for the SYCP3 core protein. (D) MYBL1 is present only in cells positive for the mid-pachytene marker H1t (asterisk), whereas earlier zygotene/pachytene spermatocytes (circled) are negative.

Mybl1 mutant testes have an aberrant transcriptome

Few targets have been identified for MYB proteins by analysis in vivo. To identify potential MYBL1-regulated genes in meiosis, we performed microarray analyses of wild-type and mutant (*Mybl1*$^{repro9/repro9}$) 14 dpp and 17 dpp testis RNA. At 14 dpp, seminiferous tubules contain spermatocytes that have advanced to early and mid-pachynema. At 17 dpp, early-mid diplotene cells appear. Many transcripts were altered twofold or more in the mutant at each time point (297 at 14 dpp and 623 at 17 dpp). However, it is likely that most of these differences are due to secondary effects of meiotic arrest, rather than to MYBL1 mutation per se.

To determine which of the 'differentially expressed' genes are specifically related to MYBL1, we subtracted genes that are commonly misregulated in 17 dpp testes of *Trip13*$^{gt/gt}$ and *Ccnb1ip1*$^{mei4/mei4}$ meiotic arrest mutants. The former is defective in noncrossover recombination repair of DSBs, and the latter specifically lacks crossing over (Li and Schimenti, 2007; Ward et al., 2007). Both mutants express MYBL1 (see above). This left 355 transcripts altered specifically in *Mybl1*$^{repro9/repro9}$ (see Table S1 in the supplementary material). One-hundred and forty of these genes were also differentially expressed in 14 dpp *Mybl1*$^{repro9/repro9}$ testes compared with wild type. The majority were downregulated (see Table S1 in the supplementary material). Semi-quantitative RT-PCR was performed on a number of the misregulated transcripts to provide orthogonal verification of the microarray results (see Fig. S5 in the supplementary material). Interestingly, X-linked genes were over-represented in the subset of upregulated genes at 17 dpp (35%). This is unique to *Mybl1*$^{repro9/repro9}$ spermatocytes, and may result from abnormal XY body formation (and thus, failure of meiotic sex chromosome inactivation, or MSCI).

To determine what pathways or classes of genes are most affected by loss of MYBL1, the 355 differentially expressed transcripts unique to *Mybl1* mutants at 17 dpp were classified according to gene ontology (GO) categories and primary cell type of expression within the testis (Fig. 6A; see Table S2 in the supplementary material). The largest number of misregulated genes are involved in nucleotide and ATP binding (44 and 37 genes, respectively), regulation of transcription (39) and cell cycle-related

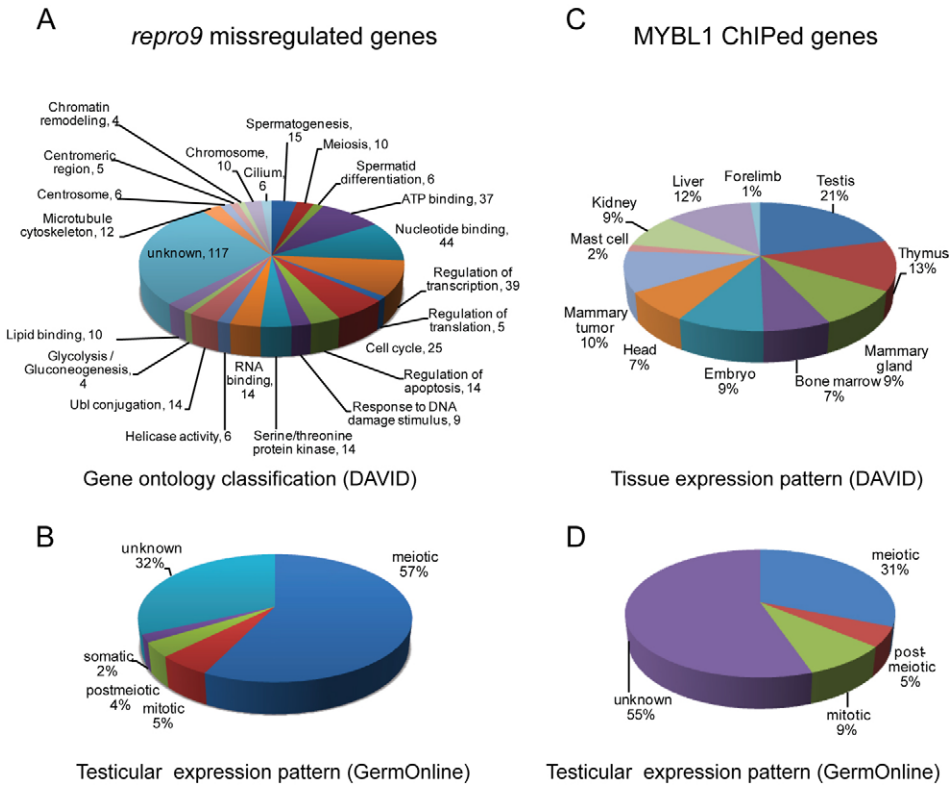

Fig. 6. Functional annotation and expression patterns of *repro9* misregulated and MYBL1 ChIPed genes. (**A**) GO classifications of transcripts specifically misregulated (subtracted versus other meiotic mutants as described in the text) in *Mybl1*^{repro9} 17 dpp testes. Analysis and annotation terms are derived from the DAVID database. (**B**) The misregulated genes in A are plotted in terms of the testicular cell type in which they are most highly transcribed in wild-type animals, according to the GermOnline database. (**C**) Plotted are the predominant sites of expression of genes identified from MYBL1 testis ChIP experiments. (**D**) Same as B but only MYBL1 ChIPed genes are plotted.

processes (25). Nine are associated with DNA repair and 10 with chromosome organization. The majority of misregulated genes are normally transcribed primarily in meiotic cells (Fig. 6B).

Identification of direct MYBL1 targets

To determine which of the differentially expressed genes are direct targets of MYBL1, we performed ChIP-chip analysis of juvenile testes by probing Nimblegen promoter arrays with DNA immunoprecipitated with the anti-MYBL1 antibody. These arrays contained probes representing 249 of the 355 genes specifically misregulated in *Mybl1*$^{repro9/repro9}$ testes (see Fig. S6 in the supplementary material). Positive signals were detected in 147 probe sets lying in proximity to 161 adjacent ('ChIPed') genes (see Table S3 in the supplementary material), 21 of which were also misregulated in the mutant testes. Taking into consideration the overall content of the two arrays (see Fig. S6 in the supplementary material), the overlap of 21 genes is highly statistically significant (representation factor: 7.9, P<2.056e-13).

MYBL1 and its paralogs can bind and transactivate MYB responsive promoter elements (Ma and Calabretta, 1994). Screening of the 147 MYBL1-bound promoter regions for transcription factor-binding sites present in the Transfac database revealed that MYB binding sites (31) were the second most prevalent after PAX4 (33). The ChIPed gene set was significantly enriched for testis expressed genes (FDR=6.6E-06; P=5.9E-09), and less so for the mammary gland (FDR=6.78E-00; P=6.3E-3) (Fig. 6C). Fifty of the 161 ChIPed genes (31%) are primarily expressed in meiotic cells (GermOnline database; Fig. 6D; see Table S4 in the supplementary material). Fourteen of the 21 genes that were both ChIPed and misregulated in *Mybl1*$^{repro9/repro9}$ testes contain consensus MYB-binding sites (Table 1).

DISCUSSION

Mutation of MYBL1, a male meiosis transcription factor

Mybl1, expressed predominantly in testis, is the least characterized of the three mammalian MYB paralogs. *Drosophila* Myb is a component of the Myb-Muv B (MMB; also known as DREAM) complex consisting of Myb and several other proteins. This complex has roles in site-specific DNA replication (Beall et al., 2002), transcriptional repression (Korenjak et al., 2004; Lewis et al., 2004) and transcriptional activation (Beall et al., 2004; Georlette et al., 2007). Whereas Myb is a transcriptional activator, other members of the complex are repressors, leading to the suggestion that the effects of MMB can switch depending on the developmental context, and that Myb functions to counter the repressive activities of MMB (Beall et al., 2007).

The *Mybl1*^{repro9} allele appears to be a separation-of-function mutation that causes a meiotic phenotype that is indistinguishable from the null, but does not cause growth retardation or defective mammary gland development, as does the null allele. The *Mybl1*^{repro9} point mutation changes a highly conserved alanine to glutamic acid (Fig. 1H) that lies near the N-terminal border of a functionally defined transactivation domain (Takahashi et al., 1995)

Table 1. Potential direct targets of MYBL1 (ChIPed and *repro9* mis-regulated genes)

Gene symbol	Gene name	log2D14	log2D17	Functional annotation	Domains
Morc2b	Microrchidia 2B	–5.81	–6.87	Unknown	ATPase-like; zinc finger; CW-type
Piwil1	Piwi-like homolog 1 (Drosophila)	–4.15	–6.85	M phase; regulation of translation; cell cycle; meiosis	Argonaute/Dicer protein; PAZ
Als2cr12	Amyotrophic lateral sclerosis 2 (juvenile) chromosome region; candidate 12 (human)	–1.22	–3.79	Unknown	n.a.
Cklf	Chemokine-like factor	–1.27	–3.02	Chemotaxis; locomotory behavior	Marvel
Cntd1	Cyclin N-terminal domain containing 1	–2.05	–2.90	Unknown	Cyclin N
Cenpp	Centromere protein P	–1.06	–1.98	Unknown	Coil-coil
Poteg	RIKEN cDNA 4921537P18 gene	–0.91	–2.86	Unknown	Ankyrin repeat
1700022c21Rik/Znrd1as	RIKEN cDNA 1700022C21 gene / ZNRD1 antisense RNA	–0.75	–2.29	Unknown	n.a.
Nol8	Nucleolar protein 8	–0.77	–1.96	Regulation of cell growth; DNA metabolic process; DNA replication	RNA recognition motif domain
Nek2	NIMA (never in mitosis gene a)-related expressed kinase 2	–0.99	–1.75	Mitotic sister chromatid segregation; M phase of mitotic cell cycle; protein amino acid phosphorylation; chromosome organization	Serine/threonine-protein kinase domain
Taf9	TATA box binding protein (TBP)-associated factor	–0.60	–1.71	Transcription	Transcription factor TAFII-31 ATPase
Moap1	Modulator of apoptosis 1	–0.17	–1.36	Apoptosis	(BH3)-like motif
P38ip	p38 interacting protein	–0.55	–1.35	Unknown	Spt20-like
4930414l22Rik/Mat2a	RIKEN cDNA 4930414L22 gene	–0.53	–1.32	Methionine metabolism	Methionine adenosyltransferase
Rpl39l	Ribosomal protein L39-like	–0.49	–1.32	Translation	Ribosomal protein L39e
Tbl2	Transducin (beta)-like 2	–0.46	–1.32	Unknown	WD40 repeat
Snx1	Sorting nexin 1	–0.51	–1.18	Intracellular protein transport	Phox homologous domain Sorting nexin; N-terminal
Ralgps2	Ral GEF with PH domain and SH3 binding motif 2	–0.17	–1.16	Small GTPase-mediated signal transduction	Pleckstrin homology domain Ras guanine nucleotide exchange factor
Hsp90aa1	Heat shock protein 90; alpha; class A member 1	–0.24	–1.12	Protein folding; nitric oxide biosynthetic process; response to unfolded protein	Heat shock protein Hsp90 InterPro IPR003594 ATPase-like
Ube2t	Ubiquitin-conjugating enzyme E2T (putative)	–0.55	–1.03	Proteolysis; protein ubiquitination	Ubiquitin-conjugating enzyme; E2
Ccnb3	Cyclin B3	0.77	1.64	Cell cycle	Cyclin

Underlined gene symbols mark genes containing MYB-binding sites in their predicted promoters.

and a Wos2 domain involved in cell cycle regulation (Munoz et al., 1999) (Fig. 1G). Interestingly, this alanine is also conserved in v-MYB and C-MYB (MYB) but not in B-MYB (MYBL2), despite being located in the least conserved region of the protein (see Fig. S7 in the supplementary material). Given that *Drosophila* Myb exists predominantly in a multi-protein complex, it is possible that the mutation affects interaction with spermatogenesis-specific, but not somatic, co-factors. Alternatively, as low amounts of MYBL1 were detected in $Mybl1^{repro9/repro9}$ testes, the mutant protein may be specifically unstable in meiotic cells.

MYBL1 deficiency disrupts expression of cell cycle genes and progression through pachynema

Mybl1-deficient spermatocytes exhibit a diverse and unique constellation of male-specific meiosis phenotypes, including aberrant chromosomal synapsis and recombination. Interestingly, they fail to display H1t deposition that is diagnostic of transition past mid-pachynema, despite the late pachytene or diplotene-like cytological appearance of some cells. Although lack of crossing over is the most remarkable and penetrant defect, it is unlikely to be the primary cause of meiotic arrest. Indeed, crossover-defective mutants such as *Mlh1*, *Mlh3* and *Ccnb1ip1* (Edelmann et al., 1996; Lipkin et al., 2002; Ward et al., 2007) die at metaphase I, presumably by triggering the spindle checkpoint (Eaker et al., 2002). Because they die before metaphase, it is likely that MYBL1-deficient spermatocytes arrest from a more proximal cause(s). One possible cause is checkpoint-mediated arrest due to DNA damage, given the fact that mutant spermatocytes display persistent SPO11-dependent RAD51 and γH2AX on synapsed chromosomes. However, the presence of DSBs on synapsed chromosomes before chiasmata formation is insufficient to block developmental progression, e.g. as in $Trip13^{Gt}$ mutants (Li and Schimenti, 2007). Another plausible explanation for spermatocyte elimination could be activation of a synapsis checkpoint, such as that which exists in *Saccharomyces cerevisiae* (Wu and Burgess, 2006). About half of mutant spermatocytes display synapsis defects, particularly

terminal asynapsis. However, limited asynapsis (e.g. that caused by presence of even multiple Robertsonian translocations) is not sufficient to arrest meiosis prior to metaphase I (Manterola et al., 2009).

Another arrest mechanism could be defective MSCI, which has been proposed to be the actual mechanism by which pervasively asynaptic mutants such as *Spo11* or *Dmc1* are eliminated (Mahadevaiah et al., 2008; Royo et al., 2010). Indeed, a subset of *Mybl1*$^{repro9/repro9}$ spermatocytes had extensive asynapsis, and those tended also to exhibit abnormal XY bodies. Possible disruption of MSCI was suggested by overexpression of some X-linked genes in the microarray data, but as half of spermatocytes had normal-appearing XY bodies intensely decorated with γH2AX, the overexpression might be attributable to only that subset with abnormal XY bodies. Notably, XY bodies of mutant spermatocytes failed to exhibit the H2A ubiquitylation that normally occurs after H2AX phosphorylation. However, histone H2A ubiquitylation is not required for silencing of sex-linked genes, and the RNF8 ubiquitin E3 ligase that plays a role in H2A ubiquitylation (Lu et al., 2010) was not downregulated in *Mybl1*$^{repro9/repro9}$ testis. Therefore, lack of H2A ubiquitylation or SUMO1 decoration of the XY body, plus the fact that mutant spermatocytes do not accumulate the mid-pachytene marker H1t, implicates a temporal disruption in pachytene progression.

Evidence has been presented that as meiotic cells enter pachynema, they switch their expression program and commit to meiotic divisions and spermiogenesis (Royo et al., 2010). However, factors that regulate this change remain unknown. Similar to duplication of spindle-pole bodies (SPBs) in yeast, in mouse this commitment is executed by regulation of centriole duplication and formation of the centrosome (Simchen, 2009). This in turn depends on timely expression of centrin 1/2 and tektin 1-5, which were all downregulated in *Mybl1* mutants. This indication of a failed progression of the meiotic program may also explain the failure of X-Y synapsis in many mutant spermatocytes. It has been shown recently that DSBs induced on the sex chromosomes are made later in prophase I (late zygonema at the earliest) than autosomes by an alternative version of the SPO11 topoisomerase (Kauppi et al., 2011).

These and other data lead us to hypothesize that a major cause of spermatocyte arrest is disruption of cell cycle progression. There is precedence for MYB-mediated cell cycle control in mammals. In particular, MYBL2 interacts with key components of the cell cycle machinery and is required for cell cycle progression in ES cells (Sala, 2005; Garcia and Frampton, 2006). In *Drosophila melanogaster*, Myb is required for the G2/M transition (Katzen et al., 1998). Because MYBL1 is primarily expressed in spermatogenesis, its potential role in cell cycle regulation has been less studied. Generally, mutations in meiotic genes that cause extensive asynapsis express little or no H1t, indicating failure to progress to mid-pachynema. By contrast, those that disrupt crossing over (such as *Mlh1*) but not synapsis do express H1t (Liebe et al., 2006; Mahadevaiah et al., 2008). As synapsis is normal in many *Mybl1*$^{repro9/repro9}$ spermatocytes, the absence of H1t and apparent arrest of pachynema progression suggest a more general cause for arrest, namely disruption of the cell cycle per se.

The expression profiling data gives more clues to support a role for MYBL1 in cell cycle progression. Among other notable *Mybl1*$^{repro9/repro}$-specific genes misregulated at 17 dpp were two cyclins (*Ccnb3* and *Ccng1*) and two NIMA (never in mitosis A) kinases (*Nek2* and *Nek4*), the orthologs of which are involved in regulating entry into mitosis (Ye et al., 1995; Wu et al., 1998). The promoters of *Ccnb3* and *Nek2* were also identified by ChIP with anti-MYBL1 (Table 1). Cyclin B3 and cyclin G1 are among the few transcripts upregulated in the *Mybl1*$^{repro9/repro9}$ mutant. CCNB3 is a pre-pachytene cyclin that is highly expressed in leptonema/zygonema and dowregulated as cells enter pachynema (Nguyen et al., 2002). Abnormal expression of CCNB3 after zygonema causes spermatogenic defects such as germ cell depletion, abnormalities of round spermatids and increased apoptosis (Refik-Rogers et al., 2006). Our data suggest that MYBL1 binding to the CCNB3 promoter (*Ccnb3* was ChIPed by anti-MYBL1 and its promoter has MYB binding sites) normally represses transcription. Because *Ccnb3* is X-linked, MSCI disruption in some cells may contribute to the elevated expression.

MYBL1 influences diverse genes and biological pathways in spermatogenesis

Although disruption of cell cycle regulation may underlie many of the observed meiotic phenotypes, examination of the genes specifically misexpressed in mutant testes indicates that MYBL1 is involved in regulating a variety of meiotic and postmeiotic functions (Fig. 6A,B; see Table S1 in the supplementary material). Interestingly, the subset downregulated at 14 dpp included several genes that, when mutated, display postmeiotic infertility phenotypes (*Meig1*, *Piwil1*, *Clgn*, *Ldhc*, *Brdt*, *Crem* and *Mak*). This indicates that crucial processes in spermiogenesis depend on regulatory mechanisms beginning in meiosis, coupled with post-transcriptional regulation that is common in haploid cells. CREM itself is an important regulator of postmeiotic gene expression (Blendy et al., 1996).

Some of the most severely downregulated transcripts are implicated in male meiosis. These include *Morc2b*, *Aym1* and *Rfx4*. *Morc2b* is one of the genes identified by ChIP, and it has been linked with *Prdm9* male infertility alleles of the histone H3 methyltransferase *Prdm9* (Hayashi and Matsui, 2006; Mihola et al., 2009). *Aym1* was identified in a screen for mouse genes that could activate promoters of early meiotic genes in *S. cerevisiae* (Malcov et al., 2004). RFX4 belongs to the regulatory factor X (RFX) family of transcription factors with testis expression that has been implicated in the regulation of spermatogenesis (Kistler et al., 2009). Interestingly, RFX4 forms a heterodimer with RFX2, encoded by a testis-specific gene that was reported to be directly transcriptionally regulated by MYBL1. The *Rfx2* promoter contains MYB-binding sites that are bound by MYBL1, its promoter can be transactivated in vitro by MYBL1 protein, and *Rfx2* transcripts are greatly reduced in *Mybl1*$^{-/-}$ testes (Morotomi-Yano et al., 2002; Horvath et al., 2009). However, our microarray analyses show only partial depletion of *Rfx2* transcripts in *Mybl1*$^{repro9/repro9}$ testes (see Fig. S5 in the supplementary material). Interestingly, one of the genes that was perturbed specifically in *Mybl1*$^{repro9/repro9}$ testes at 17 dpp was *Mlh3*, which encodes a mismatch repair protein that is required for, and serves as a marker of, crossovers in mice (Lipkin et al., 2002; Marcon and Moens, 2003). The absence of MLH3 foci may explain crossover failure in the *repro9* mutants. Some downregulated 17 dpp genes are linked to chromosome organization, including *Smc5* (a member of structural maintenance of chromosomes family) and gene encoding two centromeric proteins, *Cenpp* (also ChIPed; Table 1) and *Cenpv*. Their downregulation could potentially explain the centromeric asynapsis defects in *Mybl1*$^{repro9/repro9}$ mutants.

Overall, our data reveal the MYBL1 transcription factor as a master regulator of meiotic genes that are involved in multiple meiotic processes, including DSB repair, synapsis, crossing over,

pachytene cell cycle progression and even the expression of genes translated postmeiotically. In spite of the fact that many of the affected genes are expressed during both male and female meiosis, the regulatory roles of MYBL1 are specific to male meiosis. This underscores the remarkable differences between males and females in meiotic processes and suggests that mechanisms of gene regulation have evolved to govern both meiosis and its sexual dimorphism in mammals.

Acknowledgements
We thank E. P. Reddy for providing the *Mybl1* knockout mice, Jie Zhao for performing the microarrays and Dana Phillips for providing some RNAs for microarray analysis. This work was supported by NIH grants P01HD42137 to J.J.E., M.A.H. and J.C.S., and R01GM45415 to J.C.S. Deposited in PMC for release after 12 months.

Competing interests statement
The authors declare no competing financial interests.

Supplementary material
Supplementary material for this article is available at
http://dev.biologists.org/lookup/suppl/doi:10.1242/dev.067645/-/DC1

References

Baarends, W. M., Wassenaar, E., van der Laan, R., Hoogerbrugge, J., Sleddens-Linkels, E., Hoeijmakers, J. H., de Boer, P. and Grootegoed, J. A. (2005). Silencing of unpaired chromatin and histone H2A ubiquitination in mammalian meiosis. *Mol. Cell. Biol.* **25**, 1041-1053.
Barchi, M., Mahadevaiah, S., Di Giacomo, M., Baudat, F., de Rooij, D. G., Burgoyne, P. S., Jasin, M. and Keeney, S. (2005). Surveillance of different recombination defects in mouse spermatocytes yields distinct responses despite elimination at an identical developmental stage. *Mol. Cell. Biol.* **25**, 7203-7215.
Beall, E. L., Manak, J. R., Zhou, S., Bell, M., Lipsick, J. S. and Botchan, M. R. (2002). Role for a Drosophila Myb-containing protein complex in site-specific DNA replication. *Nature* **420**, 833-837.
Beall, E. L., Bell, M., Georlette, D. and Botchan, M. R. (2004). Dm-myb mutant lethality in Drosophila is dependent upon mip130: positive and negative regulation of DNA replication. *Genes Dev.* **18**, 1667-1680.
Beall, E. L., Lewis, P. W., Bell, M., Rocha, M., Jones, D. L. and Botchan, M. R. (2007). Discovery of tMAC: a Drosophila testis-specific meiotic arrest complex paralogous to Myb-Muv B. *Genes Dev.* **21**, 904-919.
Blendy, J. A., Kaestner, K. H., Weinbauer, G. F., Nieschlag, E. and Schutz, G. (1996). Severe impairment of spermatogenesis in mice lacking the CREM gene. *Nature* **380**, 162-165.
Cobb, J., Miyaike, M., Kikuchi, A. and Handel, M. A. (1999). Meiotic events at the centromeric heterochromatin: histone H3 phosphorylation, topoisomerase II alpha localization and chromosome condensation. *Chromosoma* **108**, 412-425.
Eaker, S., Cobb, J., Pyle, A. and Handel, M. A. (2002). Meiotic prophase abnormalities and metaphase cell death in MLH1-deficient mouse spermatocytes: insights into regulation of spermatogenic progress. *Dev. Biol.* **249**, 85-95.
Edelmann, W., Cohen, P. E., Kane, M., Lau, K., Morrow, B., Bennett, S., Umar, A., Kunkel, T., Cattoretti, G., Chaganti, R. et al. (1996). Meiotic pachytene arrest in MLH1-deficient mice. *Cell* **85**, 1125-1134.
Ganter, B. and Lipsick, J. S. (1999). Myb and oncogenesis. *Adv. Cancer Res.* **76**, 21-60.
Ganter, B., Chao, S. T. and Lipsick, J. S. (1999). Transcriptional activation by the myb proteins requires a specific local promoter structure. *FEBS Lett.* **460**, 401-410.
Garcia, P. and Frampton, J. (2006). The transcription factor B-Myb is essential for S-phase progression and genomic stability in diploid and polyploid megakaryocytes. *J. Cell Sci.* **119**, 1483-1493.
Georlette, D., Ahn, S., MacAlpine, D. M., Cheung, E., Lewis, P. W., Beall, E. L., Bell, S. P., Speed, T., Manak, J. R. and Botchan, M. R. (2007). Genomic profiling and expression studies reveal both positive and negative activities for the Drosophila Myb MuvB/dREAM complex in proliferating cells. *Genes Dev.* **21**, 2880-2896.
Handel, M. A. and Schimenti, J. C. (2010). Genetics of mammalian meiosis: regulation, dynamics and impact on fertility. *Nat. Rev. Genet.* **11**, 124-136.
Handel, M. A., Lessard, C., Reinholdt, L., Schimenti, J. and Eppig, J. J. (2006). Mutagenesis as an unbiased approach to identify novel contraceptive targets. *Mol. Cell. Endocrinol.* **250**, 201-205.
Hayashi, K. and Matsui, Y. (2006). Meisetz, a novel histone tri-methyltransferase, regulates meiosis-specific epigenesis. *Cell Cycle* **5**, 615-620.
Horvath, G. C., Kistler, M. K. and Kistler, W. S. (2009). RFX2 is a candidate downstream amplifier of A-MYB regulation in mouse spermatogenesis. *BMC Dev. Biol.* **9**, 63.
Huang, D. W., Sherman, B. T. and Lempicki, R. A. (2009). Systematic and integrative analysis of large gene lists using DAVID bioinformatics resources. *Nat. Protoc.* **4**, 44-57.
Inselman, A., Eaker, S. and Handel, M. A. (2003). Temporal expression of cell cycle-related proteins during spermatogenesis: establishing a timeline for onset of the meiotic divisions. *Cytogenet. Genome Res.* **103**, 277-284.
Kassir, Y., Adir, N., Boger-Nadjar, E., Raviv, N. G., Rubin-Bejerano, I., Sagee, S. and Shenhar, G. (2003). Transcriptional regulation of meiosis in budding yeast. *Int. Rev. Cytol.* **224**, 111-171.
Katzen, A. L., Jackson, J., Harmon, B. P., Fung, S. M., Ramsay, G. and Bishop, J. M. (1998). Drosophila myb is required for the G2/M transition and maintenance of diploidy. *Genes Dev.* **12**, 831-843.
Kauppi, L., Barchi, M., Baudat, F., Romanienko, P. J., Keeney, S. and Jasin, M. (2011). Distinct properties of the XY pseudoautosomal region crucial for male meiosis. *Science* **331**, 916-920.
Kistler, W. S., Horvath, G. C., Dasgupta, A. and Kistler, M. K. (2009). Differential expression of Rfx1-4 during mouse spermatogenesis. *Gene Expr. Patterns* **9**, 515-519.
Korenjak, M., Taylor-Harding, B., Binne, U. K., Satterlee, J. S., Stevaux, O., Aasland, R., White-Cooper, H., Dyson, N. and Brehm, A. (2004). Native E2F/RBF complexes contain Myb-interacting proteins and repress transcription of developmentally controlled E2F target genes. *Cell* **119**, 181-193.
Kotaja, N., De Cesare, D., Macho, B., Monaco, L., Brancorsini, S., Goossens, E., Tournaye, H., Gansmuller, A. and Sassone-Corsi, P. (2004). Abnormal sperm in mice with targeted deletion of the act (activator of cAMP-responsive element modulator in testis) gene. *Proc. Natl. Acad. Sci. USA* **101**, 10620-10625.
La Salle, S., Sun, F., Zhang, X. D., Matunis, M. J. and Handel, M. A. (2008). Developmental control of sumoylation pathway proteins in mouse male germ cells. *Dev. Biol.* **321**, 227-237.
Latham, K. E., Litvin, J., Orth, J. M., Patel, B., Mettus, R. and Reddy, E. P. (1996). Temporal patterns of A-myb and B-myb gene expression during testis development. *Oncogene* **13**, 1161-1168.
Lessard, C., Pendola, J. K., Hartford, S. A., Schimenti, J. C., Handel, M. A. and Eppig, J. J. (2004). New mouse genetic models for human contraceptive development. *Cytogenet. Genome Res.* **105**, 222-227.
Lewis, P. W., Beall, E. L., Fleischer, T. C., Georlette, D., Link, A. J. and Botchan, M. R. (2004). Identification of a Drosophila Myb-E2F2/RBF transcriptional repressor complex. *Genes Dev.* **18**, 2929-2940.
Li, X. C. and Schimenti, J. C. (2007). Mouse pachytene checkpoint 2 (Trip13) is required for completing meiotic recombination but not synapsis. *PLoS Genet.* **3**, e130.
Liebe, B., Petukhova, G., Barchi, M., Bellani, M., Braselmann, H., Nakano, T., Pandita, T. K., Jasin, M., Fornace, A., Meistrich, M. L. et al. (2006). Mutations that affect meiosis in male mice influence the dynamics of the mid-preleptotene and bouquet stages. *Exp. Cell Res.* **312**, 3768-3781.
Lipkin, S. M., Moens, P. B., Wang, V., Lenzi, M., Shanmugarajah, D., Gilgeous, A., Thomas, J., Cheng, J., Touchman, J. W., Green, E. D. et al. (2002). Meiotic arrest and aneuploidy in MLH3-deficient mice. *Nat. Genet.* **31**, 385-390.
Lipsick, J. S., Manak, J., Mitiku, N., Chen, C. K., Fogarty, P. and Guthrie, E. (2001). Functional evolution of the Myb oncogene family. *Blood Cells Mol. Dis.* **27**, 456-458.
Lu, L. Y., Wu, J., Ye, L., Gavrilina, G. B., Saunders, T. L. and Yu, X. (2010). RNF8-dependent histone modifications regulate nucleosome removal during spermatogenesis. *Dev. Cell* **18**, 371-384.
Ma, X. P. and Calabretta, B. (1994). DNA binding and transactivation activity of A-myb, a c-myb-related gene. *Cancer Res.* **54**, 6512-6516.
Mahadevaiah, S. K., Bourc'his, D., de Rooij, D. G., Bestor, T. H., Turner, J. M. and Burgoyne, P. S. (2008). Extensive meiotic asynapsis in mice antagonises meiotic silencing of unsynapsed chromatin and consequently disrupts meiotic sex chromosome inactivation. *J. Cell Biol.* **182**, 263-276.
Malcov, M., Cesarkas, K., Stelzer, G., Shalom, S., Dicken, Y., Naor, Y., Goldstein, R. S., Sagee, S., Kassir, Y. and Don, J. (2004). Aym1, a mouse meiotic gene identified by virtue of its ability to activate early meiotic genes in the yeast Saccharomyces cerevisiae. *Dev. Biol.* **276**, 111-123.
Manak, J. R., Wen, H., Van, T., Andrejka, L. and Lipsick, J. S. (2007). Loss of Drosophila Myb interrupts the progression of chromosome condensation. *Nat. Cell Biol.* **9**, 581-587.
Manterola, M., Page, J., Vasco, C., Berrios, S., Parra, M. T., Viera, A., Rufas, J. S., Zuccotti, M., Garagna, S. and Fernandez-Donoso, R. (2009). A high incidence of meiotic silencing of unsynapsed chromatin is not associated with substantial pachytene loss in heterozygous male mice carrying multiple simple robertsonian translocations. *PLoS Genet.* **5**, e1000625.
Marcon, E. and Moens, P. (2003). MLH1p and MLH3p localize to precociously induced chiasmata of okadaic-acid-treated mouse spermatocytes. *Genetics* **165**, 2283-2287.
Mihola, O., Trachtulec, Z., Vlcek, C., Schimenti, J. C. and Forejt, J. (2009). A mouse speciation gene encodes a meiotic histone H3 methyltransferase. *Science* **323**, 373-375.

Morotomi-Yano, K., Yano, K., Saito, H., Sun, Z., Iwama, A. and Miki, Y. (2002). Human regulatory factor X 4 (RFX4) is a testis-specific dimeric DNA-binding protein that cooperates with other human RFX members. *J. Biol. Chem.* **277**, 836-842.

Munoz, M. J., Bejarano, E. R., Daga, R. R. and Jimenez, J. (1999). The identification of Wos2, a p23 homologue that interacts with Wee1 and Cdc2 in the mitotic control of fission yeasts. *Genetics* **153**, 1561-1572.

Nguyen, T. B., Manova, K., Capodieci, P., Lindon, C., Bottega, S., Wang, X. Y., Refik-Rogers, J., Pines, J., Wolgemuth, D. J. and Koff, A. (2002). Characterization and expression of mammalian cyclin b3, a prepachytene meiotic cyclin. *J. Biol. Chem.* **277**, 41960-41969.

Oh, I. H. and Reddy, E. P. (1999). The myb gene family in cell growth, differentiation and apoptosis. *Oncogene* **18**, 3017-3033.

Refik-Rogers, J., Manova, K. and Koff, A. (2006). Misexpression of cyclin B3 leads to aberrant spermatogenesis. *Cell Cycle* **5**, 1966-1973.

Reinholdt, L., Ashley, T., Schimenti, J. and Shima, N. (2004). Forward genetic screens for meiotic and mitotic recombination-defective mutants in mice. *Methods Mol. Biol.* **262**, 87-107.

Rogers, R. S., Inselman, A., Handel, M. A. and Matunis, M. J. (2004). SUMO modified proteins localize to the XY body of pachytene spermatocytes. *Chromosoma* **113**, 233-243.

Royo, H., Polikiewicz, G., Mahadevaiah, S. K., Prosser, H., Mitchell, M., Bradley, A., de Rooij, D. G., Burgoyne, P. S. and Turner, J. M. (2010). Evidence that meiotic sex chromosome inactivation is essential for male fertility. *Curr. Biol.* **20**, 2117-2123.

Sala, A. (2005). B-MYB, a transcription factor implicated in regulating cell cycle, apoptosis and cancer. *Eur. J. Cancer* **41**, 2479-2484.

Sherman, B. T., Huang, D. W., Tan, Q., Guo, Y., Bour, S., Liu, D., Stephens, R., Baseler, M. W., Lane, H. C. and Lempicki, R. A. (2007). DAVID Knowledgebase: a gene-centered database integrating heterogeneous gene annotation resources to facilitate high-throughput gene functional analysis. *BMC Bioinformatics* **8**, 426.

Shima, J. E., McLean, D. J., McCarrey, J. R. and Griswold, M. D. (2004). The murine testicular transcriptome: characterizing gene expression in the testis during the progression of spermatogenesis. *Biol. Reprod.* **71**, 319-330.

Simchen, G. (2009). Commitment to meiosis: what determines the mode of division in budding yeast? *BioEssays* **31**, 169-177.

Smyth, G. K. (2004). Linear models and empirical bayes methods for assessing differential expression in microarray experiments. *Stat. Appl. Genet. Mol. Biol.* **3**, Article 3.

Su, A. I., Wiltshire, T., Batalov, S., Lapp, H., Ching, K. A., Block, D., Zhang, J., Soden, R., Hayakawa, M., Kreiman, G. et al. (2004). A gene atlas of the mouse and human protein-encoding transcriptomes. *Proc. Natl. Acad. Sci. USA* **101**, 6062-6067.

Takahashi, T., Nakagoshi, H., Sarai, A., Nomura, N., Yamamoto, T. and Ishii, S. (1995). Human A-myb gene encodes a transcriptional activator containing the negative regulatory domains. *FEBS Lett.* **358**, 89-96.

Toedling, J., Skylar, O., Krueger, T., Fischer, J. J., Sperling, S. and Huber, W. (2007). Ringo-an R/Bioconductor package for analyzing ChIP-chip readouts. *BMC Bioinformatics* **8**, 221.

Toscani, A., Mettus, R. V., Coupland, R., Simpkins, H., Litvin, J., Orth, J., Hatton, K. S. and Reddy, E. P. (1997). Arrest of spermatogenesis and defective breast development in mice lacking A-myb. *Nature* **386**, 713-717.

Turner, J. M., Aprelikova, O., Xu, X., Wang, R., Kim, S., Chandramouli, G. V., Barrett, J. C., Burgoyne, P. S. and Deng, C. X. (2004). BRCA1, histone H2AX phosphorylation, and male meiotic sex chromosome inactivation. *Curr. Biol.* **14**, 2135-2142.

Turner, J. M., Mahadevaiah, S. K., Ellis, P. J., Mitchell, M. J. and Burgoyne, P. S. (2006). Pachytene asynapsis drives meiotic sex chromosome inactivation and leads to substantial postmeiotic repression in spermatids. *Dev. Cell* **10**, 521-529.

Ward, J. O., Reinholdt, L. G., Hartford, S. A., Wilson, L. A., Munroe, R. J., Schimenti, K. J., Libby, B. J., O'Brien, M., Pendola, J. K., Eppig, J. et al. (2003). Toward the genetics of mammalian reproduction: induction and mapping of gametogenesis mutants in mice. *Biol. Reprod.* **69**, 1615-1625.

Ward, J. O., Reinholdt, L. G., Motley, W. W., Niswander, L. M., Deacon, D. C., Griffin, L. B., Langlais, K. K., Backus, V. L., Schimenti, K. J., O'Brien, M. J. et al. (2007). Mutation in mouse Hei10, an e3 ubiquitin ligase, disrupts meiotic crossing over. *PLoS Genet.* **3**, e139.

Wilson, L., Ching, Y.-H., Farias, M., Hartford, S., Howell, G., Shao, H., Bucan, M. and Schimenti, J. (2005). Random mutagenesis of proximal mouse Chromosome 5 uncovers predominantly embryonic lethal mutations. *Genome Res.* **15**, 1095-1105.

Wu, H. Y. and Burgess, S. M. (2006). Two distinct surveillance mechanisms monitor meiotic chromosome metabolism in budding yeast. *Curr. Biol.* **16**, 2473-2479.

Wu, L., Osmani, S. A. and Mirabito, P. M. (1998). A role for NIMA in the nuclear localization of cyclin B in Aspergillus nidulans. *J. Cell Biol.* **141**, 1575-1587.

Ye, X. S., Xu, G., Pu, R. T., Fincher, R. R., McGuire, S. L., Osmani, A. H. and Osmani, S. A. (1995). The NIMA protein kinase is hyperphosphorylated and activated downstream of p34cdc2/cyclin B: coordination of two mitosis promoting kinases. *EMBO J.* **14**, 986-994.